Research Square

Preprints are preliminary reports that have not undergone peer review.
They should not be considered conclusive, used to inform clinical practice,
or referenced by the media as validated information.

A Sustainable Hybrid Explainable AI-Based Prediction Model of Cancer Stem Cell Behavior based on Microscopic Images

Doaa Mohey Eldin

d.mohey2020@gmail.com

Research Article

Keywords: Skin Cancer, Deep Learning, Melanoma, Explainable Artificial Intelligence

Posted Date: March 3rd, 2026

DOI: https://doi.org/10.21203/rs.3.rs-8992073/v1

License: This work is licensed under a Creative Commons Attribution 4.0 International License.
Read Full License

Additional Declarations: The authors declare no competing interests.

A Sustainable Hybrid Explainable AI-Based Prediction Model of Cancer Stem Cell Behavior based on Microscopic Images

Doaa Mohey Eldin[1,*]
1Faculty of Computers and Information systems, Egyptian Chinese University, Cairo, Egypt
*Scientific Research Group in Egypt
Doaa.mohey@ecu.edu.eg
*https://egyptscience-srge.com/

Abstract: This paper presents a cancer stem cell prediction behavior system using a sustainable hybrid explainable artificial intelligence XAI-based model applied to cancer stem cell microscopic images. The proposed system integrates the XAI model in preprocessing extracted features with three enhanced transfer learning models AlexNet, GoogleNet, and ResNet50 to achieve better accuracy results of detection and classification stem cells. LIME (Local Interpretable Model-Agnostic Explanations) is used to enhance both classification accuracy and model interpretability. Experiments were conducted on three benchmark microscopic image datasets, which is (Human Against Machine with 9600 training images**).**

By cancer stem cell dataset, on the first experiment, Enhanced AlexNet, Enhanced GoogleNet, and Enhanced ResNet50 achieved classification accuracies of 85.64%**,** 88.08%, and 90.50%**,** respectively. On the second experiment, the models reached 95.15%**,** 96.06%**,** and 97.80% accuracy, respectively. Comparative analysis indicates that AlexNet consistently delivers superior performance across among datasets. By combining explainable LIME XAI technique with high-performing deep learning models, the proposed system provides a reliable and transparent solution for reliable and truth of cancer stem cell detection, supporting clinical decision-making and improving diagnostic confidence.

Keywords: Skin Cancer, Deep Learning, Melanoma, Explainable Artificial Intelligence.

1. Introduction

Cancer stem cells (CSCs) are a subset of tumor cells that persist within tumors as a distinct population. Stem cells represent an ideal source for regenerative medicine [1]. However, longitudinal assessment of stem cell phenotype and function is challenging. They drive tumor initiation, relapse, and metastasis through self-renewal and differentiation into multiple cell types, similar to typical stem cell processes [2].

Stem cells are special cells in the body that can renew themselves and differentiate into various specialized cell types [3]. They act as the body's building blocks and have the potential to repair or replace damaged tissues and organs. Stem cells are cells that haven't yet become specialized and can divide to create different types of cells in the body, like those in the heart, blood, skin, and nerves [4]. Around the world, more than 60% of stem cell research and uses are for treating cancer, helping tissues grow back, and dealing with blood-related diseases. The rest is used for conditions like brain disorders, heart problems, diabetes, and other health issues. Regenerative medicine, or stem cell therapy, has recently received a lot of attention for its tremendous potential.

Automated early prediction of cancer stem cell differentiation can significantly accelerate experimental iterations and therapeutic development. AI has emerged as a powerful tool in healthcare with numerous clinical applications of transfer learning [5].

Artificial intelligence (AI) plays a key role in helping scientists better use stem cells to identify and forecast diseases [6]. XAI [7] has grown in significance as a means of developing openness, trust, and the clinical application of deep learning models.

An Explainable AI–based Enhanced Transfer Learning (XAI-ETL) system is developed using three enhanced transfer neural networks for automated cancer stem cell detection and classification.
XAI model is designed based on LIME XAI for improving the extraction features in preprocessing phase to improve the better results in detection phase. The enhanced transfer learning model architecture becomes more adapted by removing the final fully connected layer and replacing it with a SoftMax layer initialized with random weights, making it suitable for the classification task. The main contribution lies in the introduction of an *XAI-ETL* system that combines the LIME (Local Interpretable Model-Agnostic Explanations) method with the enhanced AlexNet, GoogleNet, ResNet50.
The integration of LIME provides interpretability and feature extraction by visualizing and explaining model predictions, effectively distinguishing between cancer stem cells or not.
In addition, this system enhances cancer stem cell detection, classification, and prediction behavior via improved the feature extraction and feature selection. It demonstrates superior performance compared to other deep learning architectures, achieving improvements in accuracy, precision, recall, F1-score, and loss function.

The rest of this paper is organized as follows. A brief background about transfer learning for cancer stem cell are in section 2. The proposed method for the stem cell image detection is described in section 3. A description of the performed experiments, datasets, metrices, and the obtained results and a discussion of the proposed model are in section 4. Finally, section 5 presents the conclusion and future work in.

2. Literature review

This section explores three widely used pre-trained Transfer learning models, including AlexNet, GoogleNEt, and ResNet50 are employed for skin lesion detection and classification. These models are examined in terms of their architectural design, computational efficiency, and effectiveness in skin lesion classification tasks.

2.1 AlexNet Transfer learning model

AlexNet [8] is one of the first deep convolutional neural networks that showed how deep learning can work for image classification. AlexNet helps to find important visual details like edges, colors, and textures. Its structure includes several layers that do convolution, use ReLU activation, do pooling, and then fully connected layers. This helps it learn the differences between harmless and harmful.

2.2 GoogleNet Transfer learning model

GoogleNet [9] , also called Inception V1, is a deep convolutional neural network that uses something called the Inception module. This helps it to get different types of features from images in the same layer. When used for classifying skin lesions, GoogleNet looks at many kinds of features like edges, patterns, and shapes by using different sizes of filters, such as 1×1, 3×3, and 5×5. This helps it to find both small and big details in skin lesions, like irregular borders, different colors, and structures seen under a dermascopic. Because of its deep structure and efficient design, GoogleNet is very accurate but uses fewer parameters

than older deep networks. This makes it powerful and quick for analyzing medical images.

2.3 ResNet50 deep learning model

ResNet50 [10] enhances the training difficulty analysis based on raising the number of layers to provide a solution for the complexity of the model. Each CNN, a total of ((height(kernel)·width(kernel)·filters(input)) +1) ·filters(output)), can provide to the bill. ResNet50, a simple 7x7 kernel convolution layer via 3 channels to 32 channels, adds 4736 parameters. The neural network image input size is based on 224 by 224 by 3, and the number of classes is two, based on benign and malignant, and the number of classes is 177. CNNs can handle image-related tasks through leveraging convolutional layers that recognize patterns and hierarchies within the data.

3. The Proposed Explainable Early Melanoma Detection

The proposed model is an explainable deep learning framework that integrates LIME with three pre-trained deep neural networks, which are ResNet50, VGG16, and SqueezeNet to support the detection and classification of skin cancer. These networks are utilized for feature extraction, identifying key characteristics from input dermoscopic images, which are then stored for further analysis. To adapt the models for binary classification (benign vs. malignant), the final fully connected layers are replaced with a SoftMax classifier initialized with random weights. Additionally, an image data generator is employed to efficiently load image datasets and extract corresponding labels, streamlining the preprocessing and training workflow. Figure.1 illustrates the proposed XAI-DL framework, which is structured into four key stages including feature extraction, prediction, classification and interpretability.

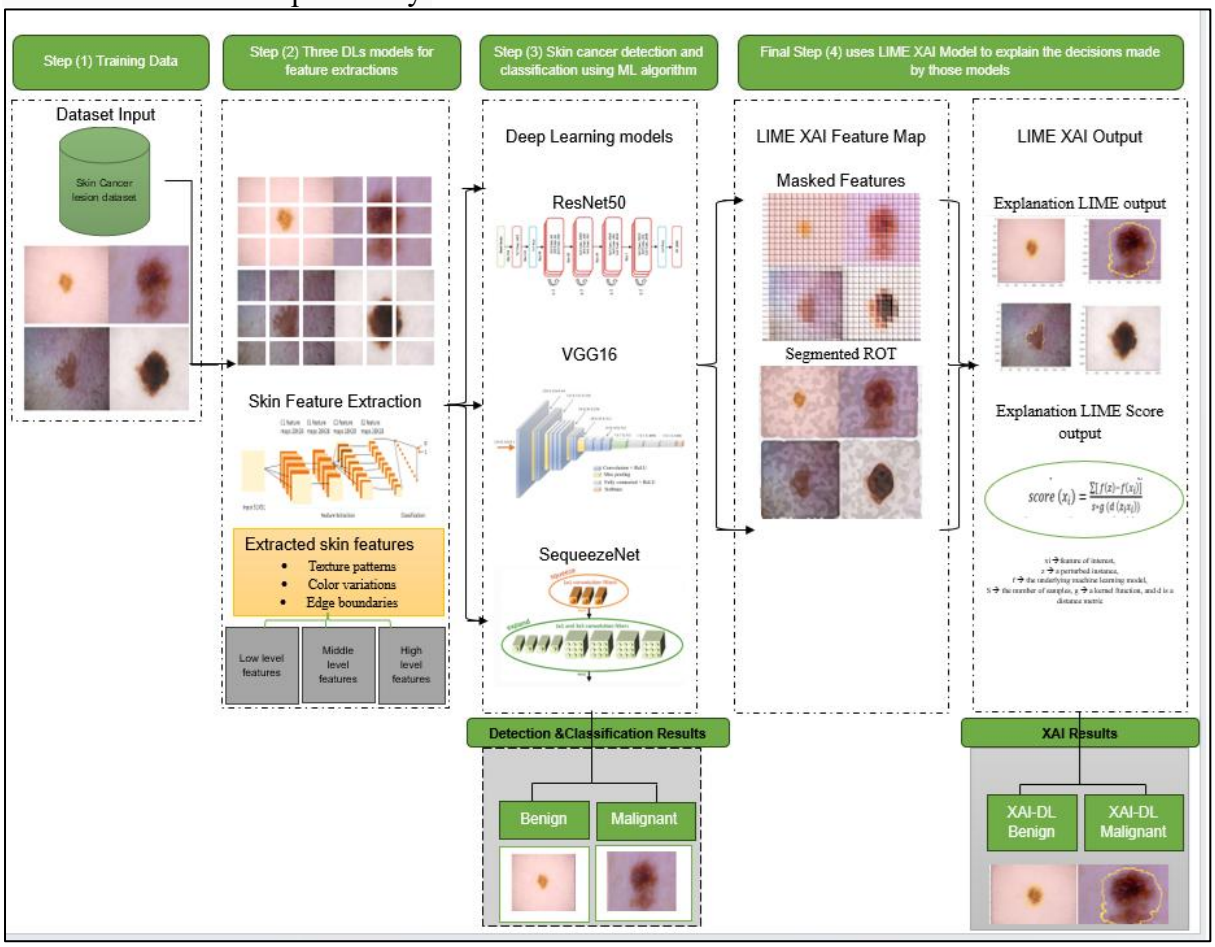


Figure.1: illustrates the proposed XAI-DL framework, which is structured into four key stages including feature extraction, prediction, classification and interpretability.

1. Train and save the pre-trained model: the model applies the training model using specified settings, measures the performance based on the diverse performance evaluation metrics, and keeps it. Prepared the dataset based on splitting the data into training and validation sets: 70% training and 30% testing.

2. Design the Deep learning model: this step applies three deep learning models for feature extraction and achieves to detect and classify the skin cancer from images. The main extracted features are texture patterns, color variations, edges and boundaries, and structural details. Texture patterns refer to the irregularities in skin surface like smoothness. Color variations differences refer to color tone like dark or light that are shown differentiating malignant from benign lesions. The skin Edges and Boundaries refers to the lesion borders and shape. The feature of structural details refers to the deep layers that can detect abstract patterns like streaks or dots. These features are analyzed into three levels, low, middle, and high levels. Low level is shown in edges and boundaries, middle level is shown in shapes and contours, and high level is shown in deep features of semantic feature patterns of skin disease.

Three deep learning models are ResNet50, VGG16, and SequeezeNet. First deep learning pre-trained Deep Residual Net (ResNet50) model is used in the proposed framework, and the model is made to fit the skin lesion melanoma-specific task by adding a layer to classify the type of skin as either benign or malignant.

Second deep learning VGG16 model is good at finding important features in medical images. VGG16 learns to recognize key aspects like the edges of a lesion, how pigments are spread, and any unusual shapes.

Third Deep learning model is SqueezeNet that is a lighter version of a neural network. It is designed to extract features in a more efficient way, using fewer parameters than models like VGG16. It has a special structure called a "fire module" that uses smaller layers with 1x1 convolutions and larger layers with both 1x1 and 3x3 convolutions. For classifying skin lesions, SqueezeNet can pick up on important details such as different colors, texture patterns, and uneven shapes. Even though it is smaller in size, it still performs well, which makes it a good option for use in mobile devices or in places where there are limited resources but quick and accurate diagnosis is needed.

3. LIME XAI Model: explains the interpretation of the features on the images to visualize the most essential features in pictures, generating both masked and binary masked pictures. LIME visualizes the interpretation to make the detection and classification more trust with feature map and Segmented ROT of each image. These evidential truth by LIME can segments the image into sections known as superpixels, breaking it down into subregions referred to as interpretable features. The default segmentation algorithm of LIME to produce these superpixels is the *quickshift* algorithm. LIME supports visualizing the picture features. LIME uses a specific method to explain how a model makes decisions for a given input.

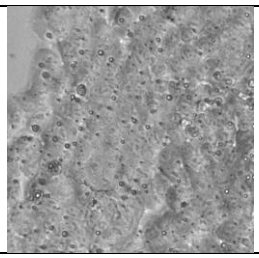
4. **Evaluation Model:** based on accuracy analysis evaluation and validation. Then showing the output of classification and the explainable graphs of classified lesions on images.

5. Experiments & results

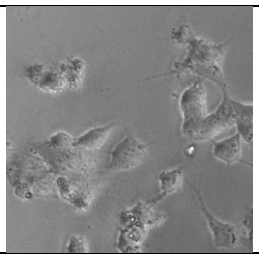
A benchmark datasets available online on Kaggle are Cancer Stem Cell (CSC) Image Dataset, was created to support interpretable AI and predictive modeling in oncology. A continuous aggressiveness score, ranging from 0 to 1, is applied to each high-resolution microscopic image

of CSCs. Instead of using traditional classification systems, these scores can be used to develop deep regression models, which represent each cell's assessed malignancy or metastasis potential. Using techniques such as Grad-CAM or LIME, this dataset aims to help researchers develop models that not only predict the potential aggressiveness of a given cancer cell but also provide an explanation of the visual characteristics that influenced this prediction. This dataset is critical for medical diagnostics due to its regression capabilities and interpretability.

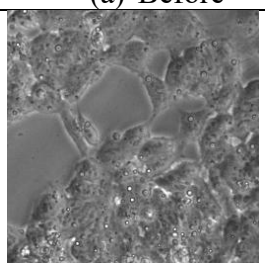
The dataset consists of 9600 images for training the model for evaluation of the model. Second dataset is called Skin Cancer MNIST: HAM10000 dataset is a popular public set of 10.015 dermatoscopic images of colored skin spots. These images are grouped into seven types of skin conditions: Actinic Keratoses, Basal Cell Carcinoma, Benign Keratoses, Dermatofibroma, Melanocytic Nevi, Melanoma, and Vascular lesions. Figure.2. Shows samples of dataset (1) and dataset (2).



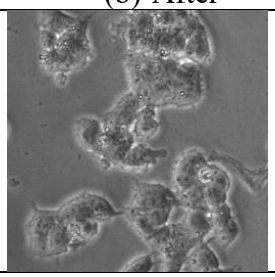
(a) Before



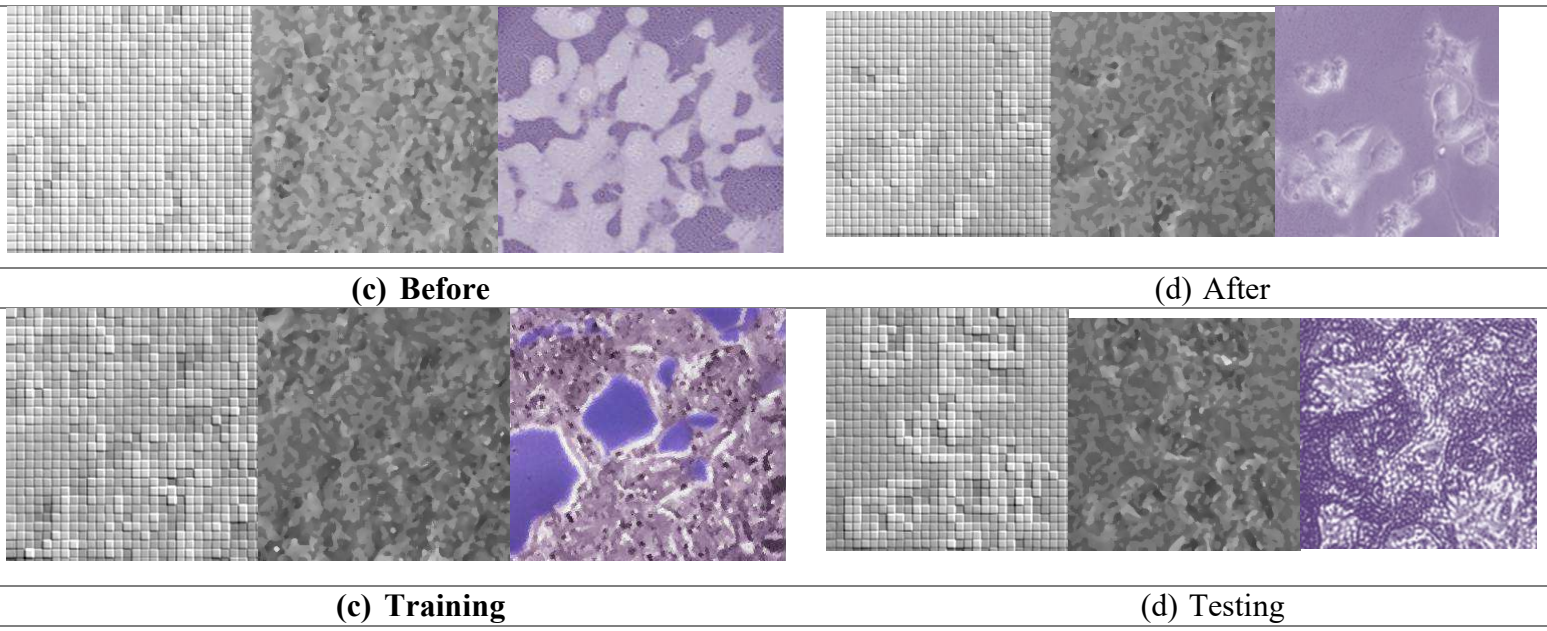
(b) After



(a) Training



(b) Testing



(c) Before (d) After

(c) Training (d) Testing

Figure.2: Example of Masked LIME XAI in a "Skin lesion melanoma malignant Vs. Benign" image classifier in dataset 1 (a) and (b) in dataset2

5.1 Validation Metrics

The performance measurement of classification of skin cancer lesion images is computed based on the precision (Pre), F1 score (F1), recall (Rec), and accuracy (Acc). Equations (1), (2), (3), and (4), and 5present their evaluation metrics equations [13]. Acc represents the right-defined subject of all identified objects. Pre represents the right-defined subject Sof all numbers of right objects. F1 is computed from recall and precision. Where TP represents true positive, TN represents true negative, FN represents false negative, and FP represents false positive.

$$Acc = \frac{TP+TN}{TP+FP+TN+FN} \quad (1)$$

$$Pre = \frac{TP}{TP+FP} \quad (2)$$

$$Rec = \frac{TP}{TP+FN} \quad (3)$$

$$F1 - measure = \frac{2*Pre*Rec}{Pre+Rec} \quad (4)$$

A loss function is an important part of machine learning and deep learning that helps measure how accurate a model's predictions are compared to the real values. It finds the difference between what the model predicts and what the actual result is during the training process as MSE loss function that shown in Equation (5). MSE refers to mean squared error, n refers to number of data points, Y_i represents observed values, and $\hat{Y_i}$ represents predicted values.

$$MSE = \frac{1}{n}\sum_{i=1}^{n}(Y_i - \hat{Y_i})^2 \qquad (5)$$

5.2 Results

a) Detection and Classification Results

For dataset 1, the experimental results of the accuracy detection and classification of ResNet50 achieves 85.66%, VGG16 archives 88.06%, and SequzeeNet achieves 88.84%, as shown in Table.1 and loss function results as shown in Table.2, as ResNet40 loss function error achieves 14.34%, VGG16 loss function error achieves 11.92%, and SequeezeNet loss function error achieves 11.16%. The number of training epochs is 5. The trained model enhances the prediction analysis on the test set to compute evaluation and validation metrics based on the loss and accuracy. Iteration per epoch: 1856; maximum number of iterations: 9280 with a learning rate of 0.0001. For dataset 2, the experimental results of the accuracy detection and classification of ResNet50 achieves 95.15%, VGG16 archives 96.06%, and SequzeeNet achieves 97.8%, as shown in Table.3 and loss function results as shown in Table.4, as ResNet40 loss function error achieves 4.85%, VGG16 loss function error achieves 3.94%, and SequeezeNet loss function error achieves 2.2%. The number of training epochs is 5. The trained model enhances the prediction analysis on the test set to compute evaluation and validation metrics based on the loss and accuracy. Iteration per epoch: 1856; maximum number of iterations: 9280 with a learning rate of 0.0001. The explanation of pervious training is shown the best deep neural network is VGG16 in training results in two datasets. Table.5 and Table.6 are shown the comparative analysis on DNNs results.

Table.1: Accuracy detection and classification for dataset 1

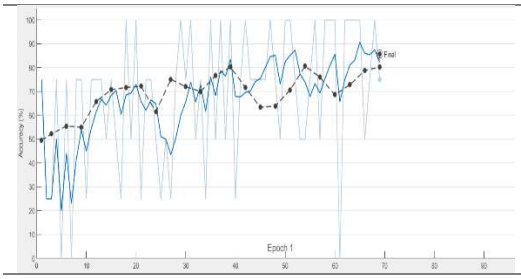
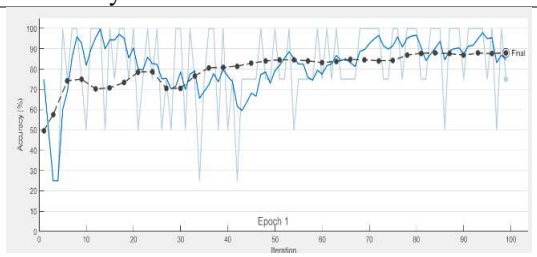
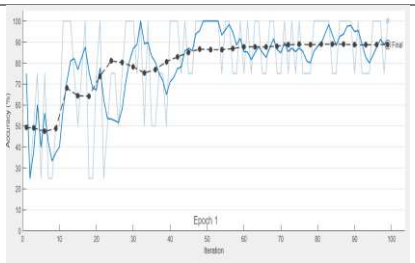
		
ResNet50 Accuracy detection 85.66%	VGG16 Accuracy detection 88.06%	SequeezeNet Accuracy 90.50 %

Table.2: loss function of the detection and classification for dataset 1

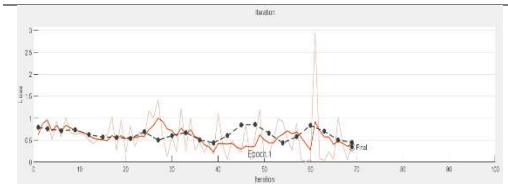
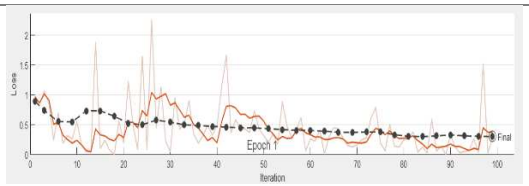
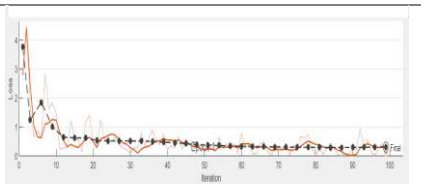
		
ResNet50 loss function (14.34%)	VGG16 loss function (11.94%)	SequzeeNet loss function (9.5%)

Table.3: Accuracy detection and classification for dataset 2

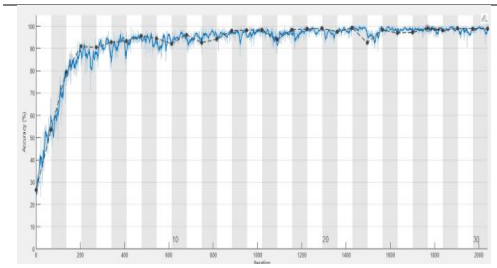
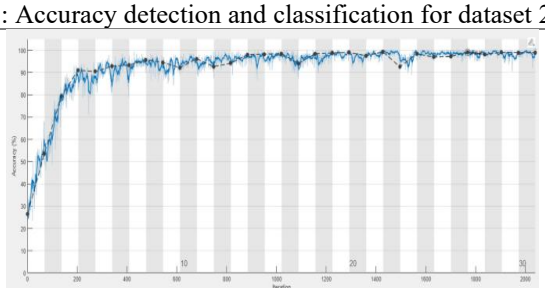
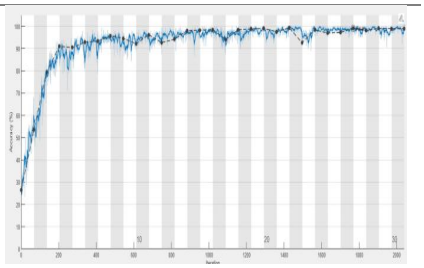
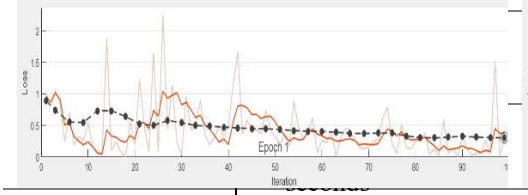
		
ResNet50 Accuracy (95.15%)	VGG16 Accuracy (96.06%)	SequeezeNet Accuracy(97.8%)

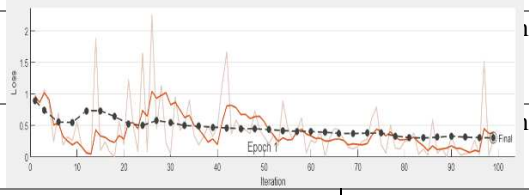
Table.5: Experimental neural networks analysis

	Dataset 1				Dataset2			
	Time amount	#Epochs	#iterations	Frequency	Time amount	#Epochs	#iterations	Frequency
ResNet50	118 minutes and 21 seconds	5	1856	3 iterations	42 minutes and 21 seconds	5	412	3 iterations

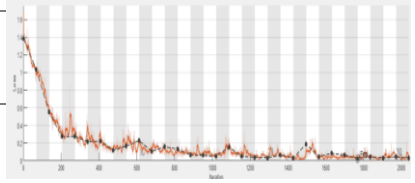
Table.4: loss function of the detection and classification for dataset 2



ResNet50 loss function (4.85 %)



VGG16 loss function (3.94%)



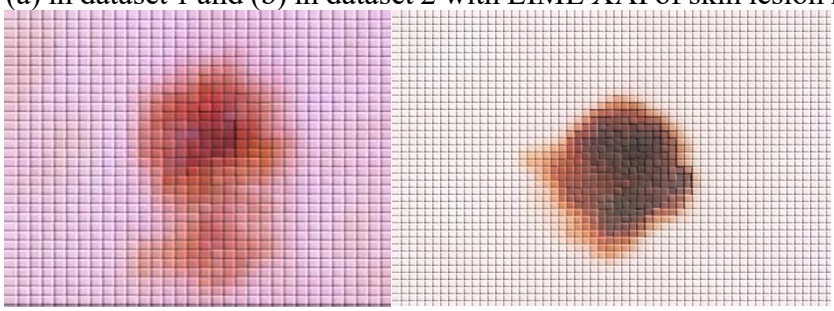
SequzeeNet loss function (2.2%)

	Dataset 1				Dataset2			
	Precision	Recall	F1-measurre	Accuracy	Precision	Recall	F1-measure	Accuracy
ResNet50	0.86	0.85	0.855	85.66%	94.9%	94.9%	94.9%	95.15%
VGG16	0.88	0.88	0.88	88.06%	95.8%	95.8%	95.8%	96.06%
SequeezeNet	0.90	0.898	0.895	90.50%	97.7%	97.7%	97.7%	97.8%.

Table.6: Accuracy detection and classification analysis results for two benchmark skin datasets

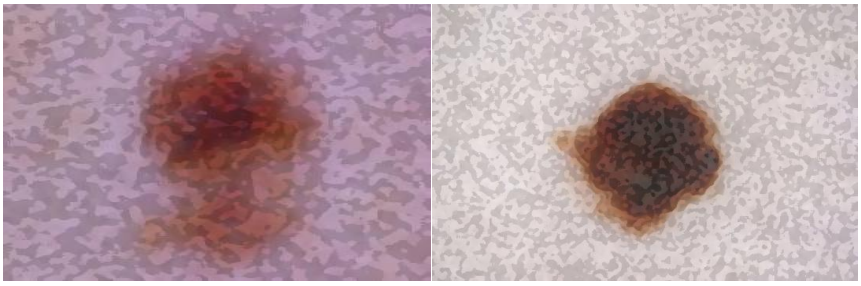
b) LIME XAI Results

Figure.3: Example of Masked LIME XAI in a "Skin lesion melanoma malignant Vs. Benign" image classifier in dataset 1 (a) and (b) in dataset2. For dataset 1: Figure.4 has two Segmented ROT samples (a) in dataset1 and (b) in dataset 2 of malignant melanoma skin lesions. Figure.5 has two examples (a) of heatmaps of malignant and benign melanoma skin lesions in dataset1 and (b) in dataset 2. Figure.6 illustrates two samples of (a) in dataset 1 and (b) in dataset 2 with LIME XAI of skin lesion melanoma.



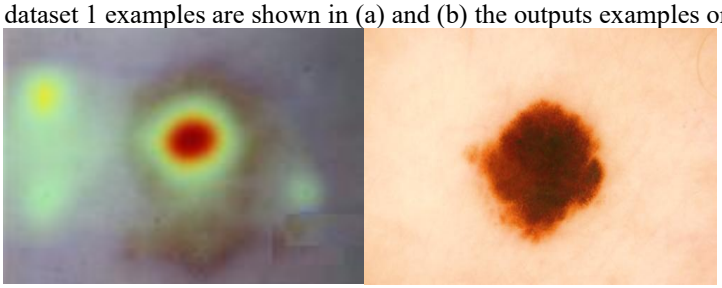
a) malignant-Masked LIME XAI b) melanoma

Figure.3: Example of Masked LIME XAI in a "Skin lesion melanoma malignant Vs. Benign" image classifier in dataset 1 (a) and (b) in dataset2.



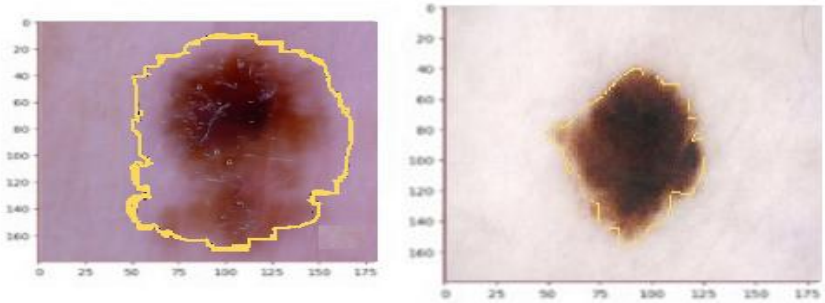
a) malignant- feature map LIME XAI b)

Figure.4: outputs of Segmented ROT based on proposed XAI Framework for skin cancer on skin lesion melanoma dataset 1 examples are shown in (a) and (b) the outputs examples on dataset2.



a) malignant-heatmap b)

Figure.5: outputs of heatmaps based on proposed XAI Framework for skin cancer on skin lesion melanoma malignant Vs. Benign dataset 1 examples are shown in (a) and the outputs examples on dataset2 (b).



a) malignant- explanation LIME XAI b) explanation LIME XAI

Figure.6: outputs of LIME explanation using XAI Framework for skin cancer on skin lesion melanoma malignant Vs. Benign dataset 1 examples are shown in (a) and (b)the outputs examples on dataset2.

The output of using LIME explanation approach for dataset1, which shows a benign skin lesion, showed that the model focuses a lot on the skin texture and the shape of the border when deciding what type of lesion it is. For an image correctly identified as "melanoma" by the model, LIME broke the lesion into six sections called superpixels. The middle part of the lesion (superpixel 1) had a strong positive score of +1. 35, meaning the unusual color pattern there strongly supported the melanoma diagnosis. Superpixel 3, which covered the uneven edge of the lesion, had a positive score of +1. 10, adding more support for a cancerous result. On the other hand, superpixel 5, which was part of the normal skin around the lesion, had a negative score of –0. 75, which slightly lowered results. Table.7 illustrates feature scores of superpixels in dataset1. Table.8 shows the Feature scores of superpixels in dataset2, Table.9 LIME Score example based on the per Superpixel for dataset1 (a) and dataset2 (b). A part of the image that was just background (superpixel 4) had a score close to 0. 00, meaning it had almost no effect. When using Equation (2), the original model confidence was 0. 92. The numerator came out to be around 200. 5. If the average of the kernel weights g(d) was 0. 4 and s was 1000, the final LIME score was approximately:

$$1000 \times 0.4200.5 \approx 0.50$$

Table.7: Feature scores of superpixels in dataset1

Superpixel	Description	Importance Score	Interpretation
1	Central irregular lesion	**+1.35**	Strong support for melanoma
2	Lesion border with asymmetry	**+1.10**	Reinforces malignant decision
3	Peripheral lesion texture	**+0.65**	Moderate positive influence
4	Background healthy skin	**–0.75**	Slight decrease in confidence
5	Neutral background patch	**0.00**	No influence
6	Hair artifact at lesion edge	**–0.90**	Distracts and reduces confidence

Superpixel 2, which is in the center-right part of the lesion, has an importance score of +1. 42. This means this smooth and even pigmented area strongly supports the idea that the lesion is a nevus, which is a benign type. Superpixel 5, which is a bit darker but still has a uniform edge, has a score of +1. 10. This further helps the model decide that the lesion is likely benign. Superpixel 1, which is in the middle of the lesion, has a score of +0.85. This suggests that the texture being consistent is a good sign for a benign diagnosis. Superpixel 6, which covers the surrounding skin and some edge artifacts, has a negative score of –0.

This slightly reduces the model's confidence in the benign classification. A small area (Superpixel 3) scored almost 0. 00, meaning it doesn't affect the result much. Some sampled predictions on perturbed images:

$$score(xi) = 1000 \cdot 0.841000 \times (-0.035) = 840 - 35 \approx -0.0417$$

Table.8: Feature scores of superpixels in dataset2

Superpixel	Region Description	Importance Score	Interpretation
1	Central smooth lesion area	+0.85	Supports benign (nevus) classification
2	Right part of lesion – uniform	+1.42	Strong positive support
3	Slight texture variation within lesion	0.00	Neutral — not influential
4	Peripheral lesion area	+0.60	Moderate support
5	Darker homogeneous border	+1.10	Positive influence on benign decision
6	Surrounding skin, hair artifact	–0.75	Negative influence — reduces confidence
7	Minor patch of skin discoloration	–0.30	Slightly contradicts benign classification

Table.9: LIME Score example based on the per Superpixel for dataset1 and dataset2

Dataset1				
Feature (Superpixel)	f(z) – $f(x_i)$	Distance d	Kernel g(d)	Score
Lesion center	–0.01	0.20	0.96	–0.0104
Lesion border	–0.05	0.45	0.82	–0.0610
Background skin	+0.02	0.33	0.89	+0.0220

Dataset2				
Feature (Superpixel)	f(z) - f(xi)	Distance **D**	Kernel g(d)g(d)g(d)	Score
Lesion center	–0.01	0.2	0.96	–0.0104
Lesion border	–0.05	0.45	0.82	–0.061
Background skin	+0.02	0.33	0.89	+0.022

6. Conclusion and Future work

The proposed XAI-DL framework is designed based on four stages, feature extraction, prediction, classification and interpretability. The deep learning is used for feature extraction of skin lesions into three levels, high, middle, and low. It also is used for detection and classification of skin cancer whether benign or malignant. It uses three deep learning models of ResNet50, VGG16, and SequeezeNet to reach better results in classification. The best detection and classification accuracy result achieves 90.50% by SequeezeNet for dataset1. The best detection and classification accuracy result achieves 97.8% by SequeezeNet for dataset2. XAI-DL uses LIME model to explain and interpret the segmented ROT to each lesion on the skin to be trust performance and make it more understandable. The LIME score achieves 0.50 to dataset1, and achieves $-0.0417$to dataset2.

For future work, apply the recommendation system based on previous results with their LIME XAI explanations. In addition, there is the benefit from the presented XAI framework for applying to diverse datasets in healthcare.

Even though AlexNet is not as deep or efficient as newer models like GoogleNet or ResNet, it is still useful for quickly getting basic features, especially in systems with limited processing power.

References

[1] K. Hauser, A. Kurz, M. Rengier, R. B. Weiss, T. Ziegelmeier, and F. Zoellner, "Explainable artificial intelligence in skin cancer recognition: A systematic review," *European Journal of Cancer*, vol. 167, pp. 248-261 (example page range), 2022, doi: 10.1016/j.ejca.2022.02.025.

[3] M. Zafar, M. Imran, M. Irfan, S. Kadry, S. Bukhari, and H. Rauf, "Skin Lesion Analysis and Cancer Detection Based on Machine/Deep Learning Techniques: A Comprehensive Survey," *Life (Basel)*, vol. 13, no. 1, p. 146, 2023, doi: 10.3390/life13010146.

[4] N. K. Mishra and M. E. Celebi, "An Overview of Melanoma Detection in Dermoscopy Images Using Image Processing and Machine Learning," arXiv:1601.07843, 2016.

[5] K. M. Hosny, M. A. Kassem, and M. M. Fouad, "Classification of skin lesions using transfer learning and augmentation with Alex-net," *PLoS One*, vol. 14, no. 5, p. e0217293, 2019, doi: 10.1371/journal.pone.0217293.

[6] M. Naqvi, S. Q. Gilani, T. Syed, O. Marques, and H. C. Kim, "Skin Cancer Detection Using Deep Learning—A Review," *Diagnostics (Basel)*, vol. 13, no. 11, p. 1911, 2023, doi: 10.3390/diagnostics13111911.

[7] O. Akinrinade and C. Du, "Skin cancer detection using deep machine learning techniques," *Intelligence-Based Medicine*, vol. 11, p. 100191, 2025, doi: 10.1016/j.ibmed.2024.100191.

[8] J. Zhou, Z. Wu, Z. Jiang, K. Huang, K. Guo, and S. Zhao, "Background selection schema on deep learning-based classification of dermatological disease," *Computers in Biology and Medicine*, vol. 149, p. 105966, 2022.

[9] M. A. Kassem, K. M. Hosny, and M. M. Fouad, "Skin lesions classification into eight classes for ISIC 2019 using deep convolutional neural network and transfer learning," *IEEE Access*, vol. 8, pp. 114822–114832, 2020.
[10] N. Natasha, M. Umar, M. K. Shahzad, S. Islam, and D. Abalo, "A deep learning approach based on explainable artificial intelligence for skin lesion classification," *IEEE Access*, vol. 10, pp. 113715–113725, 2022.
[11] H. Javed, "Melanoma Skin Cancer Dataset of 10000 Images," Kaggle, 2019. [Online]. Available: https://www.kaggle.com/datasets/hasnainjaved/melanoma-skin-cancer-dataset-of-10000-images

[12] Madar, K.S., Skin Cancer MNIST: HAM10000, Kaggle 2018. [Online]. Available: https://www.kaggle.com/datasets/kmader/skin-cancer-mnist-ham10000
[13] S. Pouyanfar, S. Sadiq, Y. Yan, H. Tian, Y. Tao, M. P. Reyes, M. L. Shyu, S. C. Chen, and S. S. Iyengar, "A Survey on Deep Learning: Algorithms, Techniques, and Applications," *ACM Computing Surveys (CSUR)*, vol. 51, no. 5, pp. 1-36, Art. no. 92, 2019, doi: 10.1145/3234150.